A MULTI-LAYER ZONE MODEL FOR PREDICTING FIRE BEHAVIOR IN A SINGLE ROOM

Keichi SUZUKI
Institute of Technology, Shimizu Corporation
3-4-17 Echujima Koto-ku, Tokyo 135-8530, Japan

Kazunori HARADA
Department of Architecture, Kyoto University
Yoshidahonmachi, Sakyo-ku, Kyoto 606-8501, Japan

Takeyoshi TANAKA
Disaster Prevention Research Institute, Kyoto University
Gokasho, Uji, Kyoto 611-0011, Japan

ABSTRACT

A multi-layer zone fire model for a single compartment was developed to predict the vertical distributions of the temperature and the gas concentrations. The basic concept of this model is to divide the fire room volume into an arbitrary number of horizontal layers, in which the temperature and other physical properties are assumed to be uniform. Considering the mass and the enthalpy flow rates through the layer interfaces and the opening and the heat transfer rates for each layer, the zone equations for the temperature and the species mass fractions are derived. The results of the sample calculations are compared with the experiments conducted by Steckler et al. From the comparison, it is considered that the model can be a practical tool to predict the behavior of fire in a room, although continuing effort may be necessary to improve the prediction.

KEY WORDS: multi-Layer zone model, fire prediction, compartment fire

1. INTRODUCTION

Recently, two types of computer-modeling methods of building fires are used in many areas of fire protection and smoke control system designing, i.e. zone models and CFD models. The zone modeling method has been successfully applied to a wide range of such purposes. It assumes that the area within a compartment consists of one layer or two, and that the physical properties of each layer, such as gas temperature and species concentrations are all uniform. In the case of the two-layer zone models, the interface of the layers changes in height according to the mass inputs through a fire plume and door jets and heat transfer [1][2][3].

The other method, computational fluid dynamics (CFD) model, predicts temperature and velocity field throughout the domain of interest. Three-dimensional time-dependent equations describing the laws of fluid dynamics are solved numerically with the surface conditions specific to the problem.

An advantage of CFD models is that they can predict detailed distributions of temperatures and velocities in the domain of interest, while zone models only give

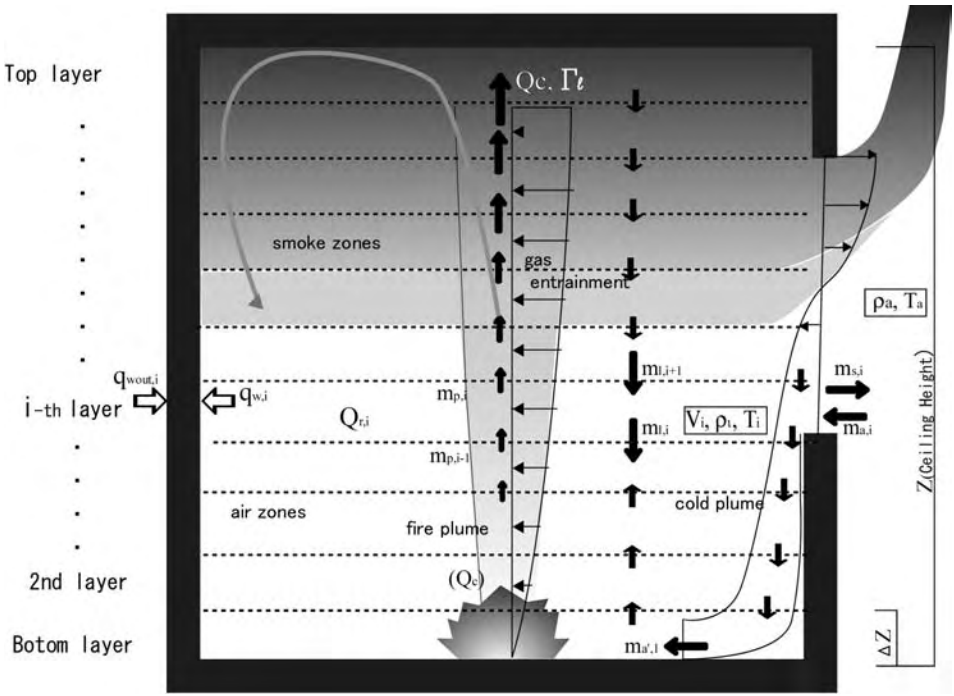

Fig.1-Illustration of the multi-layer zone model concept

average temperatures in only one layer or two assumed in a compartment. On the other hand, CFD models need tremendous CPU time. In a complicated case, it might be more than a couple of days for only 1 minute of simulation time.

In a room fire experiment, while a stratified layer situation can be observed, the layer interface is not always clear and the temperature varies rather gradually with height. So if a model which can predict the vertical temperature profile is available, more accurate analyses of fire may be made possible with a practical computation time.

In this study, a new zone modeling approach, which we call a multi-layer zone model, is addressed to predict vertical distributions of temperature and chemical species concentrations in a fire compartment. In this model the space volume in a compartment is divided into an arbitrary number of layers as the control volumes, as illustrated in Fig.1, and the physical properties, such as temperature and species concentrations, in each layer are assumed to be uniform. The boundary walls are also divided into segments in accordance with the layer division and the radiation heat transfer between the layers and between the layers and the wall segments are calculated, as well as the convective heat transfer between the layers and the wall segments. This model still retains the advantage of zone models in terms of computational burden so is expected to be useful for practical applications associated with fire safety design of buildings.

2. THE MODEL

The concept of the multi-layer zone model is demonstrated in Fig.1. One of the notable

differences of the concept of the model from the existing two-layer zone models is that the fire plume flow does not mix with the upper layer as soon as it penetrates a layer interface but continues to rise until it hits the ceiling, after which it pushes down the gases in the top layer.

2.1 Zone Conservations

The principal equations of ordinary two-layer zone models were derived from the conservation equations of mass and energy for the upper and lower layers in the compartment. In the case of the multi-layer zone model, the conservation equations for each laminated horizontal layer are also the bases to derive the equations. These conservation equations for mass, internal energy, and species fraction, are as follows:

(1) Mass conservation

$$\frac{d}{dt}(\rho_i V_i) = -\left(\dot{m}_{p,i} - \dot{m}_{p,i-1}\right) + \dot{m}_{l,i+1} - \dot{m}_{l,i} - \dot{m}_{s,i} - \dot{m}'_{a,i} \tag{1}$$

where ρ_i and V_i are the density and the volume of the i-th $(1 \le i \le n-1)$ layer, $\dot{m}_{p,i}$ is the mass flow rate at the height of layer interface of the i-th and the (i+1)-th layer inside of the fire plume. The term $\dot{m}_{p,i} - \dot{m}_{p,i-1}$ denotes the rate of mass entrained to the fire plume from the i-th layer, $\dot{m}_{l,i}$ is the net mass flow rate from the i-th layer to the (i-1)-th through the surface outside of the fire plume, $\dot{m}_{s,i}$ is the mass flow rate flowing out through the opening from the i-th layer, and $\dot{m}'_{a,i}$ is the mass gain rate of the i-th layer transported by the cold plume from the opening. For the top layer, considering that the mass rate of gas entrained into the fire plume is eventually transported to the layer, the mass conservation becomes as follows:

$$\frac{d}{dt}(\rho_n V_n) = \sum_{i=1}^{n-1}\left(\dot{m}_{p,i} - \dot{m}_{p,i-1}\right) - \dot{m}_{l,n} - \dot{m}_{s,n} - \dot{m}'_{a,n} \tag{2}$$

where subscript *n* stands for the top layer.

(2) Energy conservation

$$\begin{aligned}\frac{d}{dt}\left(C_p \rho_i V_i T_i\right) = &-C_p\left(\dot{m}_{p,i} - \dot{m}_{p,i-1}\right)T_i + C_p\left\{\max\left(\dot{m}_{l,i+1}T_{i+1}, 0\right) + \min\left(\dot{m}_{l,i+1}T_i, 0\right)\right\} \\ &- C_p\left\{\max\left(\dot{m}_{l,i}T_i, 0\right) + \min\left(\dot{m}_{l,i}T_{i-1}, 0\right)\right\} - C_p\dot{m}_{s,i}T_i + C_p\dot{m}'_{a,i}T_a - Q_{w,i} + Q_{r,i}\end{aligned} \tag{3}$$

where C_p is the specific heat, T_i is the temperature of the i-th layer, $Q_{w,i}$ is the convection heat loss to the wall surface from the i-th layer, $Q_{r,i}$ is the net radiation heat gain of the i-th layer and subscript *a* denotes the outdoor air. If $\dot{m}_{l,i+1}$ is positive, the net flow through the interface of the (i+1)-th and the i-th layers is downward, otherwise upward. The second and the third terms deal with the change of the direction of the flow with the manner as follows:

$$\max\left(\dot{m}_{l,i+1}T_{i+1}, 0\right) + \min\left(\dot{m}_{l,i+1}T_i, 0\right) = \begin{cases} m_{l,i+1}T_{i+1} & \left(m_{l,i+1} > 0\right) \\ m_{l,i+1}T_i & \left(m_{l,i+1} < 0\right) \end{cases} \quad \text{and}$$

$$\max\left(\dot{m}_{l,i}T_i, 0\right) + \min\left(\dot{m}_{l,i-1}T_i, 0\right) = \begin{cases} m_{l,i}T_i & \left(m_{l,i} > 0\right) \\ m_{l,i}T_{i-1} & \left(m_{l,i} < 0\right) \end{cases} \tag{4}$$

For the top layer, considering that the heat released by the combustion is transported to the layer through the fire plume, Q_c , the energy conservation is written as

$$\frac{d}{dt}\left(C_p\rho_n V_n T_n\right)=C_p\sum_{i=1}^{n-1}\left\{\left(\dot{m}_{p,i}-\dot{m}_{p,i-1}\right)T_i\right\} \\ -C_p\dot{m}_{l,n}T_n-C_p\dot{m}_{s,n}T_n+C_p\dot{m}'_{a,n}T_a-Q_{w,n}+Q_{r,n}+Q_c \tag{5}$$

(3) Species conservation

$$\frac{d}{dt}\left(\rho_i V_i Y_{l,i}\right)=-\left(\dot{m}_{p,i}Y_{l,i}-\dot{m}_{p,i-1}Y_{l,i-1}\right)+\left\{\max\left(\dot{m}_{l,i+1}Y_{i+1},0\right)+\min\left(\dot{m}_{l,i+1}Y_i,0\right)\right\} \\ -\left\{\max\left(\dot{m}_{l,i}Y_i,0\right)+\min\left(\dot{m}_{l,i}Y_{i-1},0\right)\right\}-\dot{m}_{s,i}Y_{l,i}+\dot{m}_{a,i}Y_{l,a} \tag{6}$$

where $Y_{l,i}$ is the mass fraction of the species *l* in the i-th layer. For the top layer, considering that the species generated by the combustion are all transported to the layer through the fire plume, the species conservation becomes as

$$\frac{d}{dt}\left(\rho_n V_n Y_{l,n}\right)=-\left(\dot{m}_{p,n}Y_{l,n}-\dot{m}_{p,n-1}Y_{l,n-1}\right) \\ -\left\{\max\left(\dot{m}_{l,n}Y_n,0\right)+\min\left(\dot{m}_{l,n}Y_{n-1},0\right)\right\}-\dot{m}_{s,n}Y_{l,n}+\dot{m}'_{a,i}Y_{l,a}+\Gamma_l \tag{7}$$

where Γ_l is the mass production rate of the species *l* by the combustion.

(4) Equation of state

Considering that a fire is basically a phenomenon at atmospheric pressure, the equation of state of the ideal gas in this model is simplified as follows:

$$\rho_i T_i = const. \tag{8}$$

2.2 Zone Governing Equations

Noting that the left-hand side of Eq.3 can be expanded as follows:

$$\frac{d}{dt}\left(C_p\rho_i V_i T_i\right)=C_p\rho_i V_i\frac{dT_i}{dt}+C_p T_i\frac{d}{dt}\left(\rho_i V_i\right) \tag{9}$$

the zone governing equation for temperature of each layer is derived by substituting Eqs.1 and 3 into Eq.9 and arranging, as follows:

$$\frac{dT_i}{dt}=\frac{1}{\rho_i V_i}\left[\left\{\max\left(\dot{m}_{l,i+1}T_{i+1},0\right)+\min\left(\dot{m}_{l,i+1}T_i,0\right)-\dot{m}_{l,i+1}T_i\right\}\right. \\ \left.-\left\{\max\left(\dot{m}_{l,i}T_i,0\right)-\dot{m}_{l,i}T_i+\min\left(\dot{m}_{l,i}T_{i-1},0\right)\right\}+\dot{m}'_{a,i}\left(T_a-T_i\right)\right]-\frac{Q_{w,i}-Q_{r,i}}{C_p\rho_i V_i} \tag{10}$$

For the top layer, substituting Eqs.2 and 5 into Eq.9 yields

$$\frac{dT_n}{dt}=\frac{1}{\rho_n V_n}\left[\sum_{i=1}^{n-1}\left\{\left(\dot{m}_{p,i}-\dot{m}_{p,i-1}\right)T_i\right\}-\left(\dot{m}_{p,n-1}-\dot{m}_{p,1}\right)T_n+\dot{m}'_{a,n}\left(T_a-T_n\right)\right]-\frac{Q_{w,n}-Q_{r,n}-Q_c}{C_p\rho_n V_n} \tag{11}$$

Likewise, the left-hand side of Eq.6 can be expanded as follows:

$$\frac{d}{dt}\left(\rho_i V_i Y_{l,i}\right)=\rho_i V_i\frac{dY_{l,i}}{dt}+Y_{l,i}\frac{d}{dt}\left(\rho_i V_i\right) \tag{12}$$

hence, the zone governing equation for mass fraction of species *l* in each layer is derived by substituting Eqs.1 and 6 into Eq.12 and arranging it as follows:

$$\frac{dY_{l,i}}{dt}=\frac{1}{\rho_i V_i}\left[\left\{\max\left(\dot{m}_{l,i+1}Y_{i+1},0\right)+\min\left(\dot{m}_{l,i+1}Y_i,0\right)-\dot{m}_{l,i+1}Y_i\right\}\right. \\ \left.-\left\{\max\left(\dot{m}_{l,i}Y_i,0\right)-\dot{m}_{l,i}T_i+\min\left(\dot{m}_{l,i}Y_{i-1},0\right)\right\}+\dot{m}'_{a,i}\left(Y_{l,a}-Y_{l,i}\right)\right] \tag{13}$$

For the top layer, substituting Eqs.1 and 7 into Eq.12 yields

$$\frac{dY_{l,n}}{dt}=\frac{1}{\rho_n V_n}\left[\sum_{i=1}^{n-1}\left\{\left(\dot{m}_{p,i}-\dot{m}_{p,i-1}\right)Y_i\right\}-\left(\dot{m}_{p,n-1}-\dot{m}_{p,1}\right)Y_n+\dot{m}'_{a,n}\left(Y_a-Y_n\right)\right]-\frac{\Gamma_l}{\rho_n V_n} \tag{14}$$

2.3. Mass Transport

Equations 10, 11, 13 and 14 can be integrated using Runge-Kutta method for the temperature and species mass fraction of each layer. However, to complete this equation system, the rate terms in the equations must be formulated based on the relevant modeling of component processes of fire. This section deals with the modeling of the mass flow rates involved.

(1) Mass flow rate through opening

Adding the energy conservation equations, Eq.3, of all layers, and Eq.5, of the top layer, we have

$$C_p\left\{\left(\sum_{i=1}^{n}\dot{m}_{a,i}\right)T_a-\left(\sum_{i=1}^{n}\dot{m}_{s,i}T_i\right)\right\}-\sum_{i=1}^{n}Q_{w,i}+\sum_{i=1}^{n}Q_{r,i}+Q_c=0 \tag{15}$$

The pressure differences between the compartment and outside at the mean height of the i-th layer from the floor, ΔP_i, is computed as

$$\Delta P_i=\Delta P-g\sum_{k=1}^{i}\rho_k dz+g\rho_a z_i \tag{16}$$

where ΔP is the pressure difference at the floor level, g is the acceleration due to gravity, dz is the thickness of layers and z_i is the mean height of the i-th layer from the floor. Then $\dot{m}_{a,i}$ and $\dot{m}_{s,i}$ are computed layer by layer, using ΔP_i as

$$\begin{cases}\dot{m}_{s,i}=\alpha_w B\ dz\sqrt{2\rho_i\Delta P_i} & (\Delta P_i\geq 0)\\ \dot{m}_{a,i}=\alpha_w B\ dz\sqrt{2\rho_a(-\Delta P_i)} & (\Delta P_i<0)\end{cases} \tag{17}$$

where α_w is the flow coefficient of the opening for the i-th layer, B is the width of the opening.

Equation 15 includes the room pressure ΔP implicitly, because $m_{a,i}$ and $m_{s,i}$ are determined as a function of ΔP. The equation can be solved for the value of ΔP using an appropriate iteration method, such as Newton-Raphson method, i.e.: starting from an initial value of ΔP and calculating $m_{a,i}$ and $m_{s,i}$ by Eq.17 and then substituting them into Eq.15, then modifying ΔP iteratively until the value of Eq.15 becomes close enough to zero.

In this model, the effect of the outdoor wind is ignored. However, in the event a simulation be made for a tall building, the effect of the wind profile with height should be considered, in which case Eq.17 still hold if Eq.16 is modified taking into account the wind effect.

A bi-directional flow at the opening will induce a negative plume because the temperature of the inflow air from outdoor is usually lower than the fire room temperature. In this model, the entrainment of the room gas into the negative plume is not considered at this moment. Instead, the mass flow through the opening is simply assumed to be transported to the lower layer if the outdoor air temperature is lower than the gas temperature of the layer by 2 Kelvin. Then, the mass flow rate into the i-th layer transported by it $\dot{m}'_{a,i}$, is calculated successively from one layer to another by the following equations.

$$\begin{cases}\dot{m}'_{a,i}=\dot{m}_{a,i} & (T_i-T_a<2)\\ \dot{m}'_{a,i}=0,\ \dot{m}'_{a,i-1}=\dot{m}_{a,i-1}+\dot{m}_{a,i} & (T_i-T_a\geq 2)\end{cases} \tag{18}$$

(2) Mass flow rate through surfaces of layers

The gas entrainment into the fire plume is important in fire predictions. In this model, the mass flow rate of the fire plume at a layer interface is assumed to be given simply by the following equation with the entrainment coefficient of fire plume C_e, regardless the temperature of the plume ambient [4]:

$$\dot{m}_{p,i} = C_e Q_c^{1/3} z_i^{5/3} \tag{19}$$

The enthalpy flow rate through the surface of the top layer to the lower layer outside of the fire plume, h_n, is obtained using Eq.8 and re-arranging Eq.5 as

$$h_n = \sum_{i=1}^{n-1} \left\{ \left(\dot{m}_{p,i} - \dot{m}_{p,i-1} \right) T_i \right\} - \dot{m}_{s,n} T_n + \dot{m}'_{a,n} T_a - \frac{1}{C_p} \left(Q_{w,n} - Q_{r,n} - Q_c \right) \tag{20}$$

The enthalpy flow rate through the interface of the (i+1)-th and the i-th layer is calculated layer by layer, using the enthalpy flow rate through the upper surface as follows:

$$h_i = -\left(\dot{m}_{p,i} - \dot{m}_{p,i-1} \right) T_i + h_{i+i} - \dot{m}_{s,i} T_i + \dot{m}'_{a,i} T_a - \frac{1}{C_p} \left(Q_{w,i} - Q_{r,i} \right) \tag{21}$$

In case h_i is a negative, the net flow through the surface is upward, otherwise downward. Thus the net mass flow rate through the surface is,

$$\begin{cases} \dot{m}_{l,i} = \dfrac{h_i}{T_i} & \left(h_i \geq 0 \right) \\ \dot{m}_{l,i} = \dfrac{h_i}{T_{i-1}} & \left(h_i < 0 \right) \end{cases} \tag{22}$$

2.4 Heat Transfer

(1) Convection heat transfer

In the compartment, the rate of the convection heat transfer from the i-th layer to the wall boundary $q_{w,i}$, is calculated as follows:

$$q_{w,i} = \alpha_c (T_i - T_{w,i,0}) A_{w,i} \tag{23}$$

where $T_{w,i,0}$ is the temperature of the wall boundary around the i-th layer, and α_c is heat transfer coefficient of the wall on the layer[kW/K/m^2], which is assumed to be as follows [5]:

$$T = \frac{T_i + T_{w,i,0}}{2} \tag{24}$$

$$\alpha_c = \begin{cases} 0.005 & \left(T \leq 300 \right) \\ 0.001(0.02T - 1) & \left(300 < T < 800 \right) \\ 0.015 & \left(800 < T \right) \end{cases} \tag{25}$$

(2) Radiation heat transfer

The radiation heat flux from each layer consists of three directional components, i.e. upward, downward and horizontal one, as shown in Fig.2. While the horizontal flux is transferred to the wall boundary, the upward and the downward radiation fluxes are exchanged between layers, with the upward flux from the top layer and the downward flux from the bottom layer as the only exceptions, where the heat fluxes are transferred to the ceiling and the floor, respectively [5].

The procedure to solve the radiation heat gain of each layer is as follows; First, calculate the heat fluxes from the floor to the bottom layer $q_{ru,0}$, then the flux from the i-

th to the upper layer $q_{ru,i}$ is calculated layer by layer from the bottom.

$$q_{ru,0} = (1-\alpha_{w,0})q_{rd,1} + \alpha_{w,0}\sigma T_{w,i,0}^4 \tag{26}$$

$$q_{ru,i} = \alpha_i F_{UL,i} q_{ru,i-1} + \alpha_i F_{UW,i}\{(1-\alpha_{w,i})q_{rw,i} + \alpha_{w,i}\sigma T_{w,i,0}^4\} + \alpha_i \sigma T_i^4 \tag{27}$$

where $q_{rw,i}$ is the heat flux from the boundary of the wall, for which the value at the last time step is used, $F_{UL,i}$ and $F_{UW,i}$ are the view factors from the upper interface to the lower interface and to the wall, α_i and $\alpha_{w,i}$ are the radiation absorptivity, which is the same as the emissivity, of the i-th layer and of the wall surface contacting with the i-th layer, respectively.

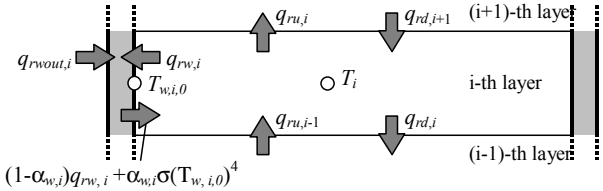

Fig.2-The directions of radiation heat flux for a layer

Next, the downward heat flux from the ceiling to the top layer $q_{rd,n+1}$, and from each layer $q_{rd,i}$, are given layer by layer from the top as follows:

$$q_{rd,n+1} = (1-\alpha_{w,n+1})q_{ru,n} + \alpha_{w,n+1}\sigma T_{w,n+1,0}^4 \tag{28}$$

$$q_{rd,i} = \alpha_i F_{LU,i} q_{rd,i+1} + \alpha_i F_{LW,i}\{(1-\alpha_{w,i})q_{rw,i} + \alpha_{w,i}\sigma T_{w,i,0}^4\} + \alpha_i \sigma T_i^4 \tag{29}$$

where $F_{LU,i}$ and $F_{LW,i}$ are the view factors from the lower surface to the upper surface and to the wall, respectively. Then $q_{rw,i}$ is obtained as follow:

$$q_{rw,i} = (1-\alpha_i)(F_{WL,i} q_{ru,i-1} + F_{WU,i} q_{rd,i+1}) + \alpha_i \sigma T_i^4 \tag{30}$$

where the values calculated at the last step are used for $q_{ru,i}$ and $q_{rd,i}$, $F_{WL,i}$ and $F_{WU,i}$ are the view factors from the wall to the lower and the upper surface. Finally, the rate of radiation heat gain of the i-th layer is calculated layer by layer, using the values of the coefficients calculated at the current time step by

$$Q_{r,i} = A_f(q_{ru,i-1} - q_{ru,i} + q_{rd,i+1} - q_{rd,i}) + A_{w,i}(q_{rw,i} - \{(1-\alpha_{w,i})q_{rw,i} + \alpha_{w,i}\sigma T_{w,i}^4\}) \tag{31}$$

It is not so easy to calculate α_i needed for these calculations because it changes according to the gas temperature and mass fractions of CO_2, H_2O and soot, still the spectra are not uniform. In this model, the Fortran program ABSORB, developed by Modak [6], is used to calculate it.

(3) Conduction heat transfer

Conduction heat transfer through the wall of the compartment is calculated, using a one-dimensional finite difference method. The governing equation is as follow:

$$\frac{\partial T_{w,i}}{\partial t} = \frac{k_w}{c_w \rho_w} \cdot \frac{\partial^2 T_{w,i}}{\partial x^2} \tag{32}$$

where $T_{w,i}$ is the temperature of the wall contacting with the i-th layer, x is the depth of the wall from the surface, t is the time, k_w, c_w and ρ_w are the thermal conductivity, the specific heat, and the density of the wall, respectively. The boundary conditions for the exposed surface and on the back of the wall are as follows:

$$-k_w \left.\frac{\partial T_{w,i}}{\partial x}\right|_{x=0} = \dot{q}_{w,i} + \dot{q}_{rw,i} \tag{33}$$

$$-k_w \left.\frac{\partial T_{w,i}}{\partial x}\right|_{x=l} = \dot{q}_{wout,i} + \dot{q}_{rwout,i} \tag{34}$$

where $\dot{q}_{wout,i}$ and $\dot{q}_{rwout,i}$ are the convection and the radiation heat flux from the outside to the back of the wall (usually negative), respectively.

2.5 Combustion

(1) Heat release rate

Heat release rate due to the combustion of the fire source is given as,

$$Q_C = \dot{m}_b \Delta H \tag{35}$$

where m_b is the mass burning rate and ΔH is the heat of combustion per unit fuel.

(2) Chemical species generation

In this model, the generation and consumption of the chemical species per unit fuel consumed in combustion are calculated by assuming a complete combustion as follows:

Fuel: $\Gamma_f = -1$

Soot: $\Gamma_{soot} = \dfrac{s}{1-w}$

O_2: $\Gamma_{O_2} = -\left\{\left(1-\dfrac{\eta}{2}\right)\dfrac{1}{12}\cdot\dfrac{W_C - w - s}{1-w} + \dfrac{1}{4}\cdot\dfrac{W_H}{1-w} - \dfrac{1}{2}\cdot\dfrac{1}{16}\cdot\dfrac{W_O}{1-w}\right\}\times 32$

CO_2: $\Gamma_{CO_2} = (1-\eta)\dfrac{W_C - w - s}{1-w}\dfrac{44}{12}$ (36)

CO: $\Gamma_{CO} = \eta\dfrac{W_C - w - s}{1-w}\cdot\dfrac{28}{12}$

H_2O: $\Gamma_{H_2O} = \dfrac{1}{2}\cdot\dfrac{W_H}{1-w}\cdot\dfrac{18}{1}$

N_2 : $\Gamma_{N_2} = \dfrac{1}{2}\cdot\dfrac{W_H}{1-w}\cdot\dfrac{28}{14}$

where w is the char fraction, s is the soot fraction, η is the rate of the carbon converted to the CO in the gas fuel, W_C , W_H and W_O are the mass fraction of C, H and O in the fuel, respectively. However, in the particular case of gaseous fuel such as methane, the value of w is naturally assumed to be zero.

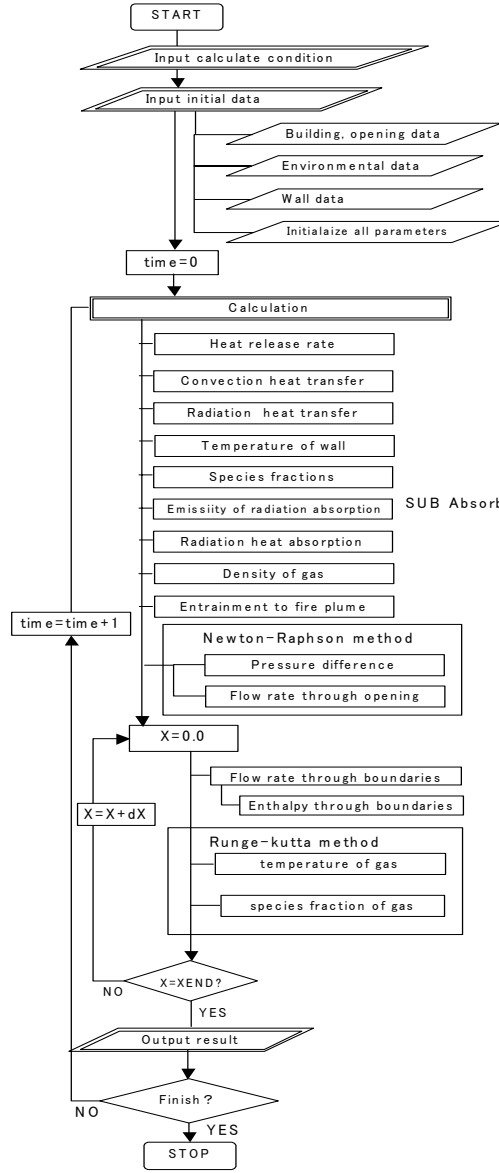

Fig.3-Flow chart of the calculation

2.6 Numerical Method

The structure of the computer program developed for numerically solving the multi-layer zone model is shown by the flow chart in Fig.3. For each time step, the zone equations for the gas temperature and species fraction of each layer are solved by Runge-Kutta method, combined with the subroutines for component physics.

3.COMPARISON WITH EXPERIMENTAL RESULTS

3.1 Experimental Data

In this section, the temperature data from 6 cases of the compartment fire experiments conducted by Steckler et al.[7] are compared with the predictions by the model. Although the experiments were for the purpose of measuring the flow rate through openings, the vertical temperature distributions were also measured accurately using aspirated thermocouples. The shape and size of the opening and the heat release rate were varied by cases. The compartment of the experiments is shown in Fig.4.

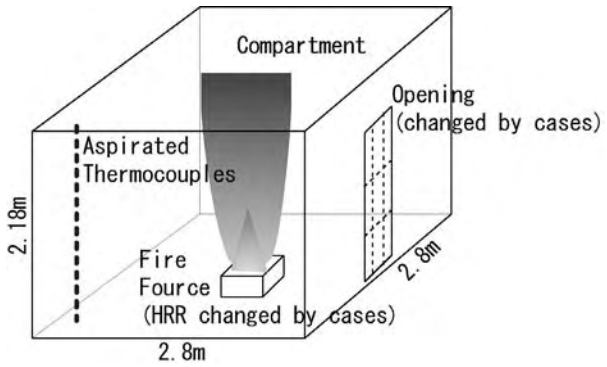

Fig.4-Compartment of the experiment

3.2 Conditions of Experiments

The lightweight walls and ceiling of the compartment (width=2.8m, depth=2.8m, height=2.18m) were lined with a ceramic fiber insulation board. Two types of openings are: door type (height=1.83m, case1:breadth=0.24m, case2-4:breadth=0.74m) and window type (breadth=0.74m, upper-height=1.83m, case5:lower-height=0.45m, case6: lower-height =1.37m) were employed in the experiments. The burner, which supplies methane at some fixed rates (equivalent to the heat release rates: 62.9, 105.3, 158kW), was installed in the center of the compartment. The thermocouple trees, each of which has 19 measurement points, were arrayed in the corner in the compartment. The temperatures were measured by aspirated thermocouples after 30 minutes from the ignition.

3.3 Condition of the Calculation

The conditions of the calculations using the multi-layer model, such as the geometry of the walls and the opening, the initial air temperature in the compartment and the heat release rate were determined basically according to the experimental conditions for each case. The room volume is divided into 18 layers. The flow rate through surfaces of layers, the temperature of gas and the species concentrations were calculated at every 0.1 second, and the flow rate through the opening, the temperature of wall, the radiation heat transfer etc. were computed at every one second. The input data of both of w and s in the Eq.36 were zero according to the property of methane.

3.4 Analysis

Fig.5 shows the vertical distribution of the temperature from the experiment at steady state stage and predictions by the model at 10 sec, 20 sec and at 1000 sec (as almost steady-state). The rectangle inserted in each figure roughly illustrates the shape of the opening at the experiment and prediction. The ordinate and the abscissa are the height and the layer temperature, respectively. The plume entrainment coefficient was set to 0.08 here, from the experimental value by Zukoski[4].

The predicted temperatures for the upper part of the room at 1000 sec. generally show satisfactory agreement with the experiments. However, (a) the temperatures in the lower part of the room are lower, and (b) the hot upper layers are thinner by 0.1-0.3m than the experiments. One of the reasons of the former(a) is that the heat release rate is assumed to be transferred the top layer without considering the radiation heat loss from the flame and the fire plume to the other layers, the wall and the floor. Another reason may be that this model neglects mixing at the layer interfaces, but a more plausible reason is that the present model has not yet incorporated the downward transport of hot gas by the negative doorjet plume.

The potential and probably the most plausible cause of (b) may be attributed to that the fire plume entrainment in the experiments is larger than that given by the assumption that C_e is 0.08. In fact, the effect of opening flow on the fire plume entrainment is extensively discussed in the report by Steckler et al.[7]. According to their data, the values of C_e were easily doubled or tripled compared with 0.08, depending on the

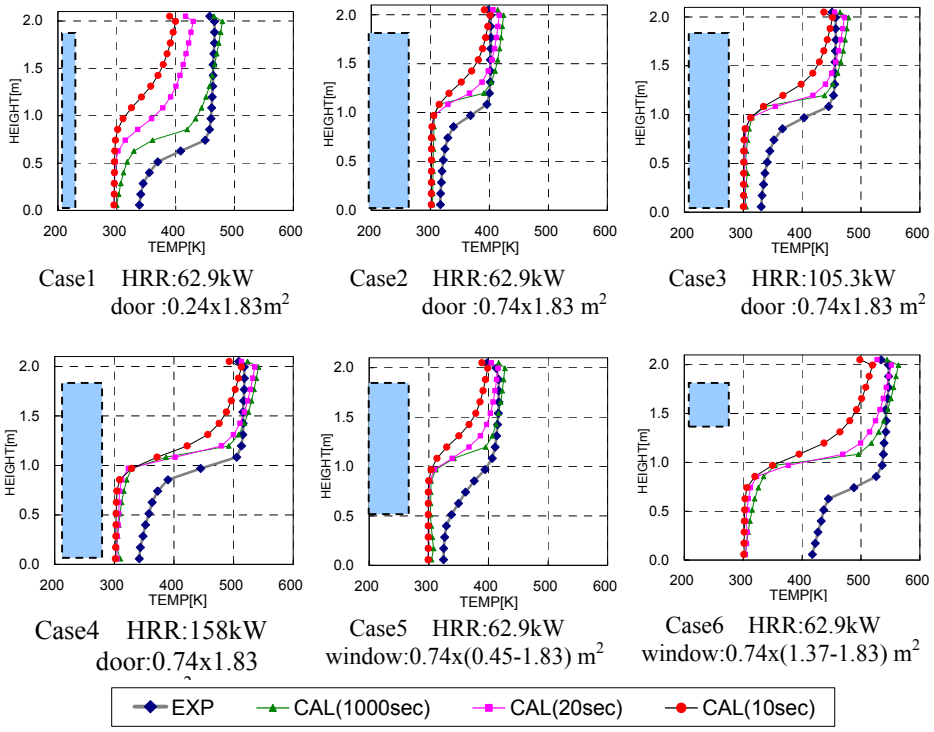

Fig.5-Comparison between experiments and predictions with time for vertical distributions of the gas temperature

location of the fire source in the room and the arrangement of the opening.

Some examples of the temperature profiles for different values of C_e, which were varied from the original 0.08 to 0.12 and 0.16, are shown in Fig. 6. As can be seen in Fig.6, the thickness of the upper layer increases as the entrainment coefficient becomes larger and the prediction and the experimental data are fairly close when the entrainment rate is doubled, particularly for the cases of door type openings. For Case 6, in which a window type opening is located at fairy upper part of the room, the agreement is still poor. This discrepancy is considered to be due to the lack of the entrainment model of the negative doorjet plume.

4. CONCLUSION

In this study, the concept and mathematical formulation of a Multi-layer zone model were introduced. Unlike the existing two-layer zone models, this model allows to predict vertical distribution of temperature and species concentrations in a fire compartment.

The results of the first stage comparison between the predictions and the experiments appear to be satisfactory and encouraging. This model is advantageous in many respects, for example, convective heat transfer to ceiling can be dealt with separately from that to vertical walls so modeling of heat transfer can be made more accurate than two layer models.

A continuing effort should be made to refine the model, particularly in the modeling of

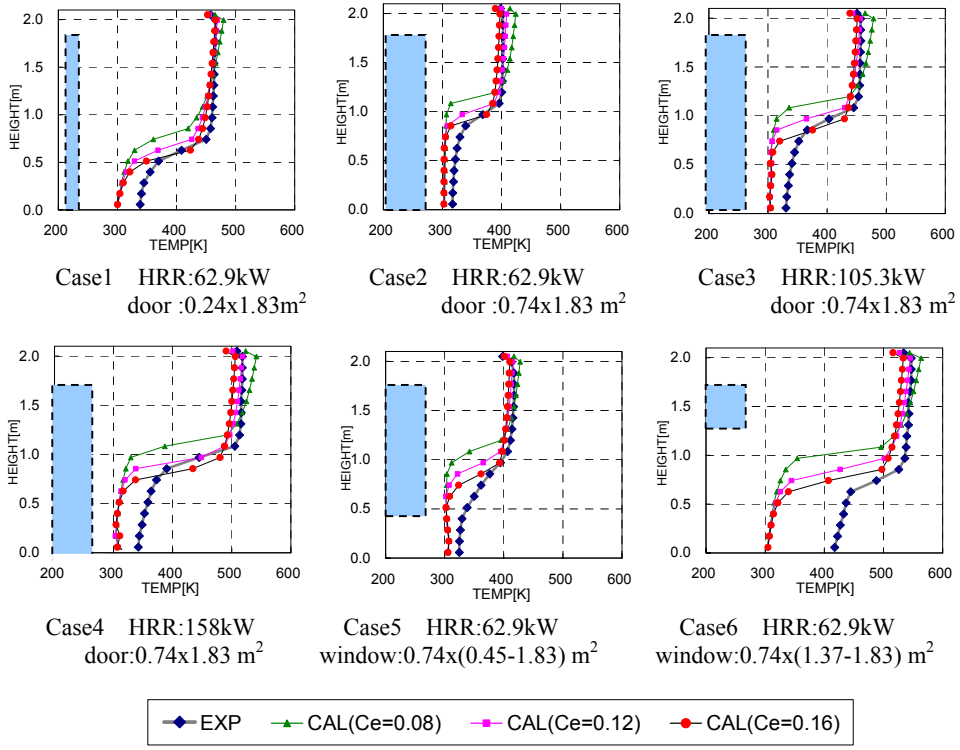

Fig.6-Comparison between experiments and predictions with three coefficients of the entrainment by the fire plume for vertical distributions of the gas temperature

negative plume which is originated from a doorjet and of radiation heat transfer from fire source and plume. Also the model should be developed to be a multi-room fire model so as to be a more viable and practical FSE tool.

REFERENCES

[1] T. Tanaka, “A Model of Multiroom Fire Spread”, NBSIR 83-2718, Nat. Bur. Stand.,Aug. 1983.
[2] Tanaka, T. and Nakamura, K., “A Model for Predicting Smoke Transport in Buildings -Base on Two Layer Zone Concept –”, Building Research Institute, No.123, BRI, MOC, 1989
[3] Fu, Z., and Hadjisphocleous G.. “A two-zone fire growth a smoke movement model for multi-compartment buildings”, Fire Safety Journal, 34 257-285, 2000.
[4] Zukoski, E. E., “Smoke Movement and Mixing in Two-Layer Fire Models”, The 8th UJNR Joint Panel Meeting on Fire Research and Safety, Tsukuba, May. 1985.
[5] Toen, C. L. Lee, K. Y. and Stretton, A. J.: “Radiation Heat Transfer”, the SFPE handbook of Fire Protedtion Engineering, 2nd Edition, Capter 4, Section 1, 1997
[6] Modak, A. T.: “Radiation from products of Combustion”, Fire Research, 1, 1978/79
[7] Steckler, K. D., Quintiere, J. G. and Rinkinen, W. J. “Flow Induced by Fire in a Compartment”, NBSIR 82-2520, Nat. Bur. Stand., Sep. 1982.